

## **A novel feature representation approach for single-lead heartbeat classification based on adaptive Fourier decomposition**

Chunyu Tan\* and Liming Zhang<sup>†</sup>

*Faculty of Science and Technology  
University of Macau, Macau, China  
\*yb57416@um.edu.mo  
†lmzhang@um.edu.mo*

Hau-Tieng Wu

*Department of Mathematics  
Duke University, Durham, NC, USA  
Department of Statistical Science  
Duke University, Durham, NC, USA  
hawwu@math.duke.edu*

Tao Qian

*Macao Center of Mathematical Sciences  
Macao University of Science and Technology  
Macao, China  
tqian@must.edu.mo*

Received 15 December 2020

Revised 18 January 2021

Accepted 20 January 2021

Published 5 March 2021

This paper proposes a novel feature representation approach for heartbeat classification using single-lead electrocardiogram (ECG) signals based on adaptive Fourier decomposition (AFD). AFD is a recently developed signal processing tool that provides useful morphological features, which are referred as AFD-derived instantaneous frequency (IF) features and differ from those provided by traditional tools. The AFD-derived IF features, together with ECG landmark features and RR interval features, are trained by a support vector machine to perform the classification. The proposed method improves the average accuracy of the feature extraction-based methods, reaching a level comparable to deep learning but with less training data, and at the same time being interpretable for the learned features. It also greatly reduces the dimension of the feature set, which is a disadvantage of the feature extraction-based methods, especially for ECG signals.

<sup>†</sup>Corresponding author.

To evaluate the performance, the Association for the Advancement of Medical Instrumentation standard is applied to publicly available benchmark databases, including the MIT-BIH arrhythmia and MIT-BIH supraventricular arrhythmia databases, to classify heartbeats from the single-lead ECG. The overall performance is compared to selected state-of-the-art automatic heartbeat classification algorithms, including one-lead and even several two-lead-based methods. The proposed approach achieves superior balanced performance and real-time implementation.

*Keywords:* Heartbeat classification; adaptive Fourier decomposition; instantaneous frequency; time–frequency representation.

AMS Subject Classification 2020: 92C55, 42A38, 92A12

## 1. Introduction

Cardiovascular disease (CVD) is the leading cause of death globally. According to a report of the American Heart Association in 2020, CVDs claimed 17.8 million lives in 2017, and this number amounted to an increase of 21.1% from 2007.<sup>32</sup> Among the various CVDs, arrhythmia accounts for a large proportion, and early diagnosis of arrhythmia is of great significance to healthcare professionals.<sup>28</sup>

Electrocardiogram (ECG) is an effective, noninvasive and well-established diagnostic tool for arrhythmia. Long-term monitoring is required to achieve early diagnosis of life-threatening arrhythmias. Thanks to the advances in technology, this can be achieved by wearable Holter monitors or mobile devices.<sup>12,15</sup> As the manual diagnosis of recorded long-term ECG signals is time consuming and prone to errors, a reliable computerized interpretation of ECG,<sup>27</sup> or at least computer-aided automatic heartbeat classification, has become increasingly important. Our focus in this study is computer-aided automatic heartbeat classification. Although several commercial automatic heartbeat classification algorithms have been proposed, in general, these exhibit substantial misdiagnosis rates,<sup>27</sup> even when they are applied to the multiple-lead ECG used in hospitals. Moreover, the performance is clearly deteriorated when only a single-lead ECG is used, as it is more challenging to determine the delineation of fiducial points. Wearable Holvers and mobile devices that are commonly used for early diagnosis of arrhythmia are usually equipped with single-lead ECG.<sup>28</sup> Thus, it is necessary to develop an accurate automatic heartbeat classification algorithm for single-lead ECG.

Successful heartbeat classification usually comprises three important procedures: preprocessing, feature extraction and classification. Automatic heartbeat classification algorithms can be divided into two main categories based on the manner in which these three steps are carried out. The first category includes methods based on feature extraction and classifier training, while the second category includes those based on black box deep learning approaches.<sup>2,16</sup>

Feature selection and dimension reduction are key processes in feature extraction-based classification. An effective feature extraction method can not only simplify the computation, but also provide superior classification performance. The ECG features commonly employed for classification tasks are based

on ECG landmarks.<sup>11,36</sup> Researchers have also considered transform domain features based on discrete cosine transform,<sup>7</sup> principal component analysis,<sup>3,34</sup> independent component analysis (ICA)<sup>34</sup> and so on. Another set of features focuses on the non-stationarity of the ECG, and researchers have taken the ECG time–frequency representation into account.<sup>17</sup> The above-mentioned features are usually used in combination, resulting in a higher dimensionality of the feature set. Large feature dimensions lead to high computational costs, making real-time implementation in wearable Holters, mobile devices and off-the-person sensors impractical.

Deep learning offers an integrated scheme that combines feature extraction and classification. Acharya *et al.*<sup>2</sup> and Zubair *et al.*<sup>38</sup> developed 9-layer and 3-layer convolutional neural network (CNN) methods, respectively, whereas, Yildirim<sup>35</sup> constructed the deep bidirectional long short-term memory network-based wavelet sequences model. Deep learning-based methods generally exhibit higher accuracy rates; for example, the average accuracy rates were 93.47% in Ref. 2 and 99.25% in Ref. 35. However, a large amount of training data is required for training deep neural networks (NNs). The benchmark datasets in the standard MIT-BIH arrhythmia database are not sufficiently large to support such training.<sup>16</sup> To solve this problem, artificial synthetic data<sup>2</sup> and the intra-patient paradigm have been used in Refs. 2, 35 and 18, which reduce the reliability of the methods. Some methods also use additional classifiers, such as support vector machine (SVM) and decision tree,<sup>18</sup> to improve the final accuracy after CNN. Moreover, several methods only focused on some specific classes and ignore the others, as in Ref. 22, in which the application of the restricted Boltzmann machine (RBM) and deep belief network (DBN) is used for detecting ventricular and supraventricular heartbeats, thereby achieving high performance in those two classes, while the other classes perform poorly.

As ECG signals are always imbalanced, the deep learning-based classification methods, even the feature extraction-based methods are prone to ineffective due to the small amount of abnormal data. However, the main focus of the ECG classification is to identify the abnormal classes, rather than the normal class. From the clinical perspective, balanced classification results are sought.

In this paper, we propose a new automatic heartbeat classification method for single-lead ECG signals with rigorous mathematical support, which belongs to the first category. Our approach uses the time–frequency features of the ECG signal to perform feature extraction. Popular time–frequency representation methods in the literature include short-time Fourier transform (STFT),<sup>19</sup> the Wigner–Ville distribution,<sup>1</sup> wavelet transform<sup>3,34</sup> and synchrosqueezing transform.<sup>17</sup> Ambiguity is inevitably caused by the uncertainty principle<sup>26</sup> in STFT,<sup>19</sup> which may mask important heartbeat information. Moreover, the Wigner distribution<sup>1</sup> suffers from the cross-term problem.<sup>37</sup> To the best of the authors' knowledge, no STFT or Wigner distribution-based ECG feature representation method for heartbeat classification is available in the literature. In wavelet transform, the selections of the mother wavelet

and number of decomposition levels are problematic. While synchrosqueezing transform<sup>17</sup> may aid in eliminating above problems, the computational complexity is nontrivial, making it unsuitable for real-time implementation. Therefore, we consider a new type of time–frequency analysis, based on adaptive Fourier decomposition (AFD)<sup>25,37</sup> to address the limitations of the aforementioned time–frequency analysis approaches.

AFD is a novel signal processing technique with a rigorous mathematical foundation, which generalizes the traditional Fourier decomposition by considering the Blaschke decomposition (BKD) theory in the complex analysis.<sup>8,9,30</sup> It decomposes a given signal by adaptively selecting its associated basis from the Takenaka–Malmquist (TM) system.<sup>21,29</sup> By achieving the maximal energy gain in each decomposition iteration, AFD decomposes a signal into several constitutional components known as *mono-components*. Those mono-components possess positive instantaneous frequencies (IFs) and no intersection occurs among any of the IFs.<sup>10,37</sup> The positive IFs effectively reflect the time-varying characteristics of the signals, such as the morphology of the heartbeats. The discriminating ability of these IF features is sufficient to exceed the performance levels of other methods using complex feature screening and assessment processes. A balanced classification performance is achieved by these features for abnormal heartbeats detection.

The contributions of this study are as follows:

- New AFD-derived IF features are introduced for the first time in application and heartbeat classification in the literature. It significantly reduces the feature dimensions of ECG signals for feature extraction-based approaches.
- The proposed method can be implemented automatically and in real time using a low-power platform. Our classification requires only a small amount of training data compared to deep learning methods. These advantages offer significant potential for practical use in wearable Holters, mobile devices and off-the-person sensors (provided that a high-quality ECG signal is available), and even for user-side learning training in the near future.
- An inter-patient cross-validation (CV) paradigm is applied to the entire data in the benchmark database to validate the proposed method. The results are more stable and reliable compared to those methods using intra-patient or using selected data from the database.
- The experiment results show that our method reaches over 80% balanced accuracy classification rates on overall and all four classes, which is the best balanced result in the literature on heartbeat classification.

The rest of this paper is organized as follows. The proposed method is described in detail in Sec. 2. In Sec. 3, the results of the classification performance and the performance comparisons with state-of-the-art algorithms are presented. Several concerned issues are discussed in Sec. 4. Finally, conclusion is drawn in Sec. 5.

## 2. Methods

In this section, we first present the mathematical foundation of the proposed approach. Then the new time–frequency feature representation-based ECG classification system is described in detail. Finally, the databases and the assessment strategies are introduced.

### 2.1. Mathematical foundation

#### 2.1.1. AFD-based time–frequency representation

Take a real-valued function  $s \in L^2(\partial\mathbb{D})$ , where  $\partial\mathbb{D}$  is the unit circle. The associated analytic signal  $s^+$  is defined as  $s^+ = \frac{1}{2}(s + iHs + c_0)$ , where  $c_0$  is the 0th Fourier coefficient and  $H$  is the Hilbert transform. For the analytic signal  $s^+$ , AFD conducts rapid converging approximation of  $s^+$  in orthogonal terms, of the form

$$s_{\text{rec}}^+ = \sum_{n=1}^N c_n B_n, \quad (2.1)$$

under selection of the parameters  $a_1, \dots, a_N$ , by the maximal selection principle.<sup>25</sup>  $a_1, \dots, a_N \subset \mathbb{D}$ , where  $\mathbb{D} \subset \mathbb{C}$  is the unit disc,  $B_n(z) = \frac{\sqrt{1-|a_n|^2}}{1-\bar{a}_n z} \prod_{k=1}^{n-1} \frac{z-a_k}{1-\bar{a}_k z}$ ,  $n \in \mathbb{N}$  are modified Blaschke products of the TM system,<sup>21,29</sup> and  $c_n = \langle s^+, B_n \rangle$  is the  $n$ th coefficient of  $B_n$ .  $N \in \mathbb{N}$  is known as the *decomposition level* and  $s_{\text{rec}}^+$  is referred as the *AFD approximation of degree  $N$* . We have  $s^+ = s_{\text{rec}}^+ + R_N$ .  $R_N$  is the remainder after  $N$  times decomposition, which represents the error between  $s^+$  and  $s_{\text{rec}}^+$ . It was proven in Ref. 25 that  $s_{\text{rec}}^+$  converges to  $s^+$  in the  $H^2$  convergence sense; that is,  $\|R_N\|_{H^2} \rightarrow 0$  as  $N \rightarrow \infty$ . Refer to Fig. 1 for a detailed illustration of AFD for the ECG signal.

Then

$$s_{\text{rec}} = 2\Re s_{\text{rec}}^+ - c_0, \quad (2.2)$$

where  $\Re$  means taking the real part, and  $s_{\text{rec}}$  is the approximation of  $s$ . When  $s$  is an ECG signal, refer to Fig. 2 for examples when  $N = 10$ .

It is natural to consider a time–frequency representation to visualize the oscillation of a given real-valued signal  $s$ . We denote  $c_n B_n$ ,  $n = 1, \dots, N$  as the  $n$ th level AFD of  $s$ . If  $c_n B_n(e^{it}) = \rho_n(t) e^{i\theta_n(t)}$ , where  $t \in [0, 2\pi)$  is the time, the *transient time–frequency representation* of  $s$ , as proposed in Refs. 37 and 10, can be defined as

$$R_s(t, \zeta) = \sum_{n=1}^N \rho_n^2(t) \delta(\theta'_n(t)), \quad (2.3)$$

where  $\zeta > 0$  is the frequency and  $\delta$  is the distributional Dirac function.<sup>10</sup> Note that  $R_s$  can be numerically plotted as an image for the purpose of visualization, as illustrated in Fig. 1.

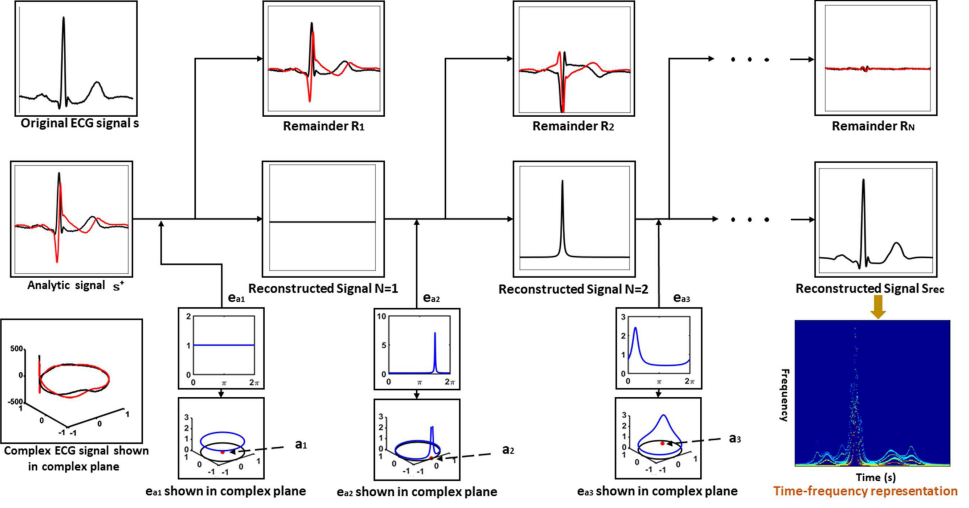


Fig. 1. Flowchart of AFD with real ECG signal. The black and red curves denote the real and imaginary parts of a complex signal, respectively. Note that  $a_l$ , where  $l = 1, 2, 3$ , are indicated as red dots in those plots illustrating  $e_{a_l}$ . In the time–frequency representation in the bottom-right subplot, note that the IFs of all decomposed components are grouped together (color online).

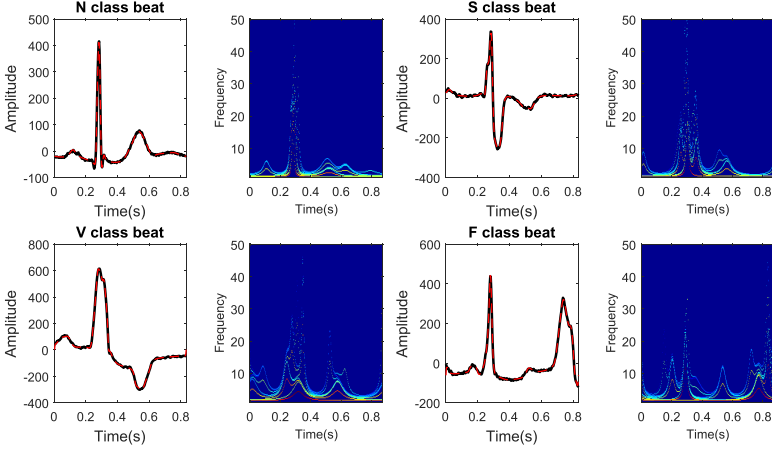


Fig. 2. Results of AFD approximation and associated time–frequency representations of four different heartbeat classes. The decomposition level is  $N = 10$ . The black lines represent the original heartbeats, while the red dotted lines represent the respective approximations (color online).

### 2.1.2. IF feature

A function  $s(e^{it}) = \rho(t)e^{i\theta(t)} \in L^2(\partial\mathbb{D})$  is known as a *mono-component* if  $\rho \geq 0$  and  $\theta' \geq 0$  a.e.<sup>37</sup>; that is, it has well defined, non-negative analytic phase derivatives. The non-negative analytic phase derivative  $\theta'$  is the IF of  $s$ . According to (2.1)

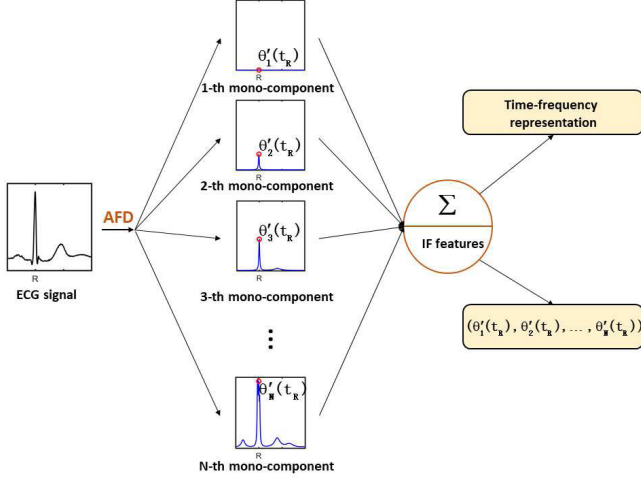


Fig. 3. Process of extracting IF feature vectors.  $(\theta'_1(t_R), \theta'_2(t_R), \dots, \theta'_N(t_R))$  are IF features in our method.

and (2.3), if  $c_n B_n(e^{it}) = \rho_n(t)e^{i\theta_n(t)}$ , by direct calculation, we obtain

$$\theta'_n(t) = \frac{|a_n| \cos(t - \theta_{a_n}) - |a_n|^2}{1 - 2|a_n| \cos(t - \theta_{a_n}) + |a_n|^2} + \sum_{l=1}^{n-1} \frac{1 - |a_l|^2}{1 - |a_l| \cos(t - \theta_{a_l}) + |a_l|^2}, \quad (2.4)$$

where  $\theta_{a_n} = |a_n|e^{i\theta_{a_n}}$ . We view the IF function  $\theta'_n$  as a feature of the given signal. In our application, if  $t_R$  represents the location of an R-peak, we refer to  $\theta'_n(t_R)$  as the  $n$ th R-peak IF feature of that heartbeat. For the decomposition level  $N$ , we refer to the vector  $(\theta'_1(t_R), \theta'_2(t_R), \dots, \theta'_N(t_R))$  as the R-peak IF feature vector of a given heartbeat. The process of extracting the R-peak IF feature vectors is described in Fig. 3.

## 2.2. AFD-based heartbeat classification system

The proposed automatic heartbeat classification system consists of three steps: preprocessing, feature extraction and classifier construction. In the first step, the raw ECG signals are divided into heartbeat segments following the standard R-peak detection algorithm. Thereafter, AFD is applied to generate the IF feature vector for each heartbeat segment. A set of commonly applied landmark features, including the QRS duration, R-peak amplitude and RR interval, is also derived. Finally, the SVM classifier is trained for the purpose of classification. An illustration of the proposed algorithm is provided in Fig. 4.

### 2.2.1. Preprocessing

The preprocessing stage consists of R-peak detection and heartbeat segmentation. As the R-peak detection is not the focus of this work, the R-peak annotations

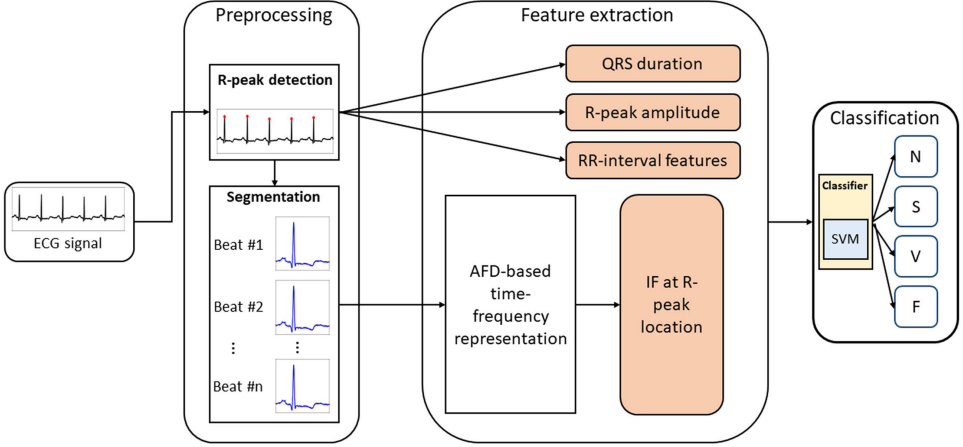


Fig. 4. Overview of proposed automatic heartbeat classification algorithm.

provided in the MIT-BIH arrhythmia database are used for the heartbeat segmentation. For each detected R-peak, 100 sampling points before the R-peak location and 200 sampling points thereafter are selected to construct an associated heartbeat segmentation. Considering that the sample rate is 360 Hz, a heartbeat segment is approximately 0.83 s.

### 2.2.2. Feature extraction

AFD is applied to every heartbeat segment, with the decomposition level  $N = 10$  because 10 decomposed mono-components can effectively recover the heartbeat segment. Therefore, each heartbeat segment is decomposed into nine mono-components, as the first mono-component is trivial according to the selection of  $a_1 = 0$ . The IFs of these nine mono-components at the R-peak locations are selected as features of each heartbeat segment; that is, the R-peak IF feature vector is  $(\theta'_2(t_R), \theta'_3(t_R), \dots, \theta'_{10}(t_R)) \in \mathbb{R}^9$ , as illustrated in Fig. 3. The distributions of the nine R-peak IF features of the N, S, V and F classes are graphically represented in Fig. 5. According to Fig. 5, we can observe that the IF feature vectors are discriminative representations of the heartbeat classes. Moreover, landmark features and dynamic features that have been clinically studied with stipulated diagnostic standards are selected. In total, we have 14 features for each heartbeat segment, which are listed in Table 1.

### 2.2.3. Classifier

We consider the widely applied classifier with a solid theoretical foundation, namely the kernel SVM,<sup>31</sup> to establish the heartbeat classification model, owing to its strong performance, as reported in previous works for classifying beat types. Numerically,



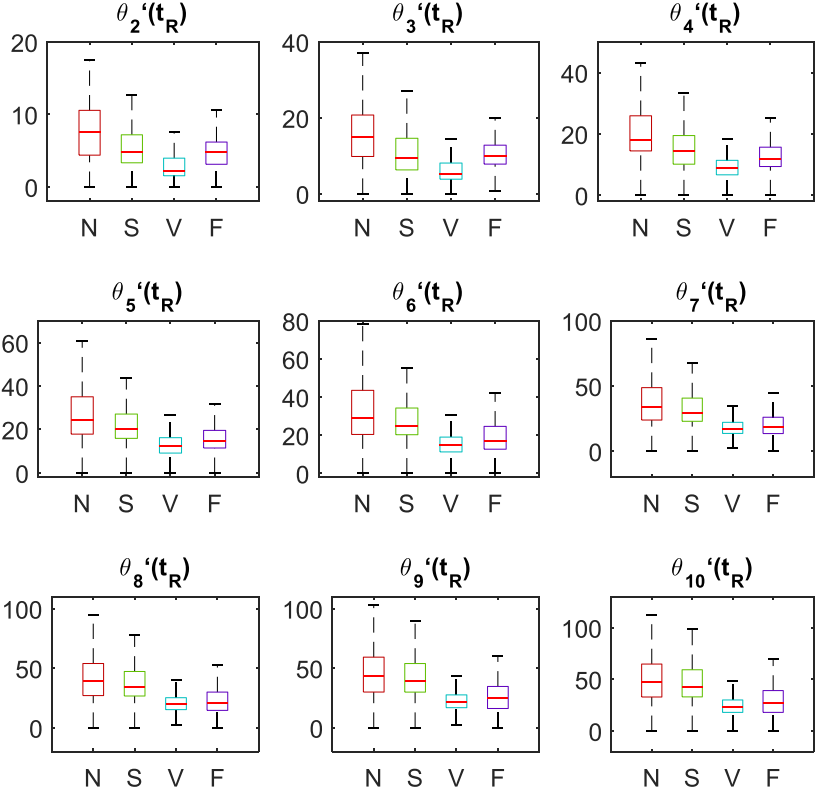


Fig. 5. Boxplots of IF distribution of nine mono-components obtained by AFD at R locations for main beat types presented in MIT-BIH database. Note that we set all  $a_1 = 0$  for  $N = 1$ , resulting in  $\theta_1'(t_R) = 0$  for each heartbeat segment, so we omit it. N: N class; S: S class; V: V class; F: F class.

Table 1. Feature set in this study.

Features	Description
R-peak IF feature vector	AFD-derived IFs at R-peaks
QRS duration	Duration of QRS complex
R-peak amplitude	Amplitude of R point location
Pre-RR interval	Time difference between current and previous beat at R-peak
Post-RR interval	Time difference between current and next beat at R-peak
Local-RR interval	Average R-peak to R-peak interval over 10 beats

the LIBSVM library<sup>6</sup> is applied to implement the kernel SVM. The weighted SVM classifier is trained, as the training data from the MIT-BIH arrhythmia database is imbalanced. Specifically, we assign each class a weight to penalize the class according to its prevalence in order to relieve the problem generated by the imbalance of the training dataset.

### 2.3. Databases

The well-known MIT-BIH arrhythmia database<sup>a</sup> from PhysioNet<sup>14</sup> is used for evaluating the proposed method. The database contains 48 recordings, each of which lasts about 30 min, with two leads: lead A and lead B. In 45 recordings out of 48, lead A is modified lead II (MLII), while lead B is mainly V1, but sometimes V2, V4 or V5; in the remaining three recordings, lead A is V5 and lead B is V2 or II. The signals are sampled at 360 Hz. In this work, we use lead A for the automatic heartbeat classification. The database includes expert annotations. The annotations follow the Association for the Advancement of Medical Instrumentation (AAMI) standard,<sup>4,5</sup> which further categorizes the beat types into different classes, as indicated in Table 2. In particular, the N class contains beats originating from the sinus node (normal and bundle branch block beat types); the S class contains supraventricular ectopic beats; the V class contains ventricular ectopic beats; the F class contains beats resulting from fusing normal and ventricular ectopic beats and the Q class contains unknown beats, including paced beats. In this work, the Q class is discarded according to the recommended practice, as it is marginally represented in the database. The provided expert annotations are used as the standard to evaluate the performance of the classification results.

In addition to the MIT-BIH arrhythmia database, the MIT-BIH supraventricular database<sup>b</sup> is used to alleviate the imbalanced class issue when using the MIT-BIH arrhythmia database. Specifically, limited beats of type S exist in the MIT-BIH arrhythmia database. The MIT-BIH supraventricular database consists of 78 recordings of approximately 30 min each, sampled at 128 Hz with two leads. In this study, the ECG recordings from MIT-BIH supraventricular database are resampled to 360 Hz to match the sampling rate of the MIT-BIH arrhythmia database.

### 2.4. Assessment strategies

#### 2.4.1. Inter-patient CV

CV is applied to evaluate the performance of the proposed algorithm. Based on different types of CV, heartbeat classification methods can be divided into two categories, namely intra-patient CV and inter-patient CV. When the training and testing sets contain heartbeats from the same subjects, the CV is known as intra-patient CV; otherwise, it is known as inter-patient CV.<sup>11,17,33</sup> Intra-patient CV has been widely adopted and can achieve optimistic results.<sup>2,3,18,35</sup> However, we cannot retrain the heartbeat signals of every new patient in practice. Due to numerous variations in ECG signals, the intra-patient CV-based methods may not be able to predict the heartbeat classification of unknown patients, therefore it is not suitable for the actual situation. For inter-patient CV, heartbeats in the training set and the testing set are from different patients so that inter-subject variations are taken

<sup>a</sup><http://www.physionet.org/physiobank/database/mitdb/>.

<sup>b</sup><http://www.physionet.org/physiobank/database/svdb/>.

Table 2. Relationships between heartbeat types and heartbeat classes in MIT-BIH arrhythmias database, and corresponding training and test data numbers.

Heartbeat types	N	L	R	A	a	J	S	V	F	e	j	E	Total
Heartbeat classes	N	N	N	S	S	S	S	S	F	N	N	V	Q
All records	74,173	8038	7233	2535	149	84	2	6730	801	14	223	106	15
DS1	37,917	3933	3764	807	99	33	2	3648	423	14	12	105	8
DS2	36,256	4105	3469	1728	50	51	0	3082	378	0	211	1	7

*Note:* N: normal; L: left bundle branch block; R: right bundle branch block; A: atrial premature; a: aberrated atrial premature; J: nodal (junctional) premature; S: supraventricular premature or ectopic; V: premature ventricular contraction; F: fusion of ventricular and normal; e: atrial escape; j: nodal (junctional) escape; E: ventricular escape; Q: unclassifiable beat. DS1 represents the training data number, while DS2 represents the test data number. DS1 contain heartbeats from records 101, 106, 108, 109, 112, 114, 115, 116, 118, 119, 122, 124, 201, 203, 205, 207, 208, 209, 215, 220, 223 and 230. DS2 contains heartbeats from records 100, 103, 105, 111, 113, 117, 121, 123, 200, 202, 210, 212, 213, 214, 219, 221, 222, 228, 231, 232, 233 and 234.

into account, providing a more realistic evaluation for heartbeat classification. Following the state-of-the-art approaches,<sup>11,17,33</sup> inter-patient CV is performed in this study.

#### 2.4.2. Assessment metrics

The confusion matrix is used in this study that shows the detailed distribution of the classification results achieved by a classifier. Besides, the following assessment metrics are also employed. We denote  $n_{kl}$  as the  $(k, l)$ th entry of the confusion matrix. The sensitivity (Se), positive predictivity ( $+P$ ) for the  $k$ th class are defined as

$$\text{Se}_k = \frac{n_{kk}}{\sum_{l=1}^N n_{kl}}, \quad +P_k = \frac{n_{kk}}{\sum_{k=1}^N n_{kl}}. \quad (2.5)$$

Larger Se and  $+P$  value reflect better classification performance for the  $k$ th class. The overall accuracy (Acc) is denoted as

$$\text{Acc} = \frac{\sum_{k=1}^N n_{kk}}{\sum_{k=1}^N \sum_{l=1}^N n_{kl}}. \quad (2.6)$$

### 3. Results

In this section, we give detailed results of time–frequency feature images, imbalanced classification results, balanced classification results and comparison results with other state-of-the-art methods.

#### 3.1. Time–frequency features images

Figure 2 presents the results of four heartbeat segments from different classes, including the AFD approximation of degree 10 and their respective time–frequency representations. In addition, Fig. 6 provides detailed time–frequency features of the V class heartbeat given in Fig. 2.

#### 3.2. Imbalanced results

The entire MIT-BIH arrhythmia database is divided into a training set (DS1) and a test set (DS2) according to the recommendation in Ref. 11, that is, DS1 contains all heartbeats in 22 records and DS2 contains all heartbeats in the other 22 records. The records in DS1 and DS2 do not cross each other. The remaining four records containing paced beats are removed. Table 2 illustrates the detailed heartbeat distribution for different heartbeat classes in DS1 and DS2.

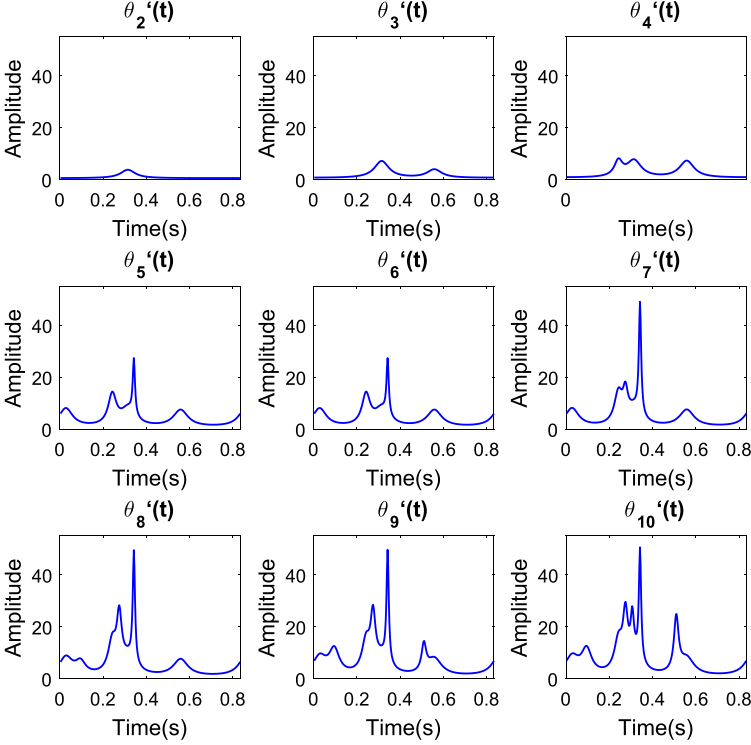


Fig. 6. The detailed time–frequency features of the V class heartbeat in Fig. 2.

The imbalance model means that the imbalance of the data is not taken into account. Since most heartbeats in the database are normal heartbeats, the accuracy of the overall and normal heartbeat classification is higher, and the accuracy of the abnormal heartbeat classification is lower. In imbalance model, the classifier is trained on all features listed in Table 1 and the heartbeats from DS1. The optimal parameters for the kernel SVM are determined by the grid optimization method, by applying 10-fold CV. Once the optimal parameters are selected, the established SVM classifier is validated on DS2.

The optimal parameters for the kernel SVM classifier determined from DS1 are  $C = 2.8$ ,  $\sigma = 0.0008$ . The confusion matrix is presented in Table 3. This classifier assessed on DS2 achieves an overall Acc of 94.7% and N class Se of 99.1%. As indicated in Table 3, the performance of the S class and F class is poor, mainly owing to the imbalanced dataset issue.

### 3.3. Balanced results

In order to improve the accuracy of abnormal heartbeat classification, we add the following operations to the imbalance model: extend DS1 with the S class in the

Table 3. Confusion matrix of imbalance model.

		Predicted			
		N	S	V	F
Reference	N	43,642	94	304	1
	S	1076	454	298	1
	V	443	10	2630	0
	F	321	1	44	12

Table 4. Confusion matrix of balance model.

		Predicted			
		N	S	V	F
Reference	N	37,681	3555	231	2574
	S	299	1470	58	2
	V	67	433	2477	106
	F	38	7	20	313

MIT-BIH supraventricular database, add the P-wave IF features of each heartbeat in the training features, and provide weights for different heartbeat classes. As the last few mono-components can better reflect the subtle oscillations of ECG signals, for each heartbeat segment, the IFs at the 50th samples before the R-peak location of the last five mono-components refer as the P-wave IF feature vector, that is,  $(\theta'_6(t_R - 50), \theta'_7(t_R - 50), \dots, \theta'_{10}(t_R - 50)) \in \mathbb{R}^5$ . Therefore, there are five more features used in balance model. In this case, the accuracy of overall and normal heartbeat classification rates may be reduced, but the accuracy of abnormal heartbeats will be greatly improved. In balance model, the classifier is trained on the extended DS1, and assessed on DS2.

In balance model, the optimal parameters for the weighted SVM classifier are determined as  $C = 3$ ,  $\sigma = 0.0006$ ,  $\omega_1 = 0.42$ ,  $\omega_2 = 36$ ,  $\omega_3 = 2.5$  and  $\omega_4 = 1.79$ , where  $\omega_1$ ,  $\omega_2$ ,  $\omega_3$  and  $\omega_4$  are the weights for classes N, S, V and F, respectively. The confusion matrix is presented in Table 4, the final performance of the classifier tested on DS2 exhibits an overall Acc of 85.02% and Se of all classes over 80%. The detailed Se and  $+P$  values of each class are provided in Table 5. Note that this model achieves a more balanced result, and the results of the S class and F class are improved.

### 3.4. Performance comparison

A comparison of the classification accuracy between the proposed method and the state-of-the-art methods based on inter-patient CV is provided in Table 5. All methods shown in Table 5 used all data of the MIT-BIH arrhythmia database for training and validating, complied with the AAMI standard and followed DS1 and DS2 division schemes proposed in Ref. 11. Except Refs. 38 and 22 are deep

Table 5. Comparisons of the proposed method with other state-of-the-art methods under the inter-patient CV.

Method	# Leads	# Features	N		S		V		F	
			Se	+P	Se	+P	Se	+P	Se	+P
Zubair <i>et al.</i> <sup>38</sup>	1	–	96.8	97.23	35.08	44.65	79.19	64.26	61.02	54.5
Mathews <i>et al.</i> <sup>22</sup>	1	26	86.14	99.27	70.99	32.44	85.22	55.27	67.19	10.76
De Chazal <i>et al.</i> <sup>11</sup>	2	52	86.9	99.2	75.9	38.5	77.7	81.9	89.43	0.08
Llamedo and Martinez <sup>20</sup>	2	39	77.55	<b>99.47</b>	76.46	41.34	82.94	87.97	<b>95.36</b>	4.23
Ye <i>et al.</i> <sup>34</sup>	2	132	88.5	97.5	60.8	52.3	81.5	63.1	19.6	2.5
Herry <i>et al.</i> <sup>17</sup>	1	6	83.13	98.93	<b>81.14</b>	31.93	77.50	79.05	83.25	6.91
Chen <i>et al.</i> <sup>7</sup>	1	33	98.4	95.4	29.5	38.4	70.8	85.1	0	0
Mathews <i>et al.</i> <sup>23</sup>	1	104	95.9	98.2	78.1	49.7	<b>94.7</b>	93.9	12.4	23.6
Zhang <i>et al.</i> <sup>36</sup>	2	46	88.9	99.0	79.1	36.0	85.5	92.8	93.8	13.7
Proposed method										
(Imbalanced results)	1	14	<b>99.1</b>	96.0	24.8	<b>81.2</b>	85.3	<b>94.7</b>	3.2	<b>85.7</b>
(Balanced results)	1	19	85.56	98.94	80.37	26.9	80.34	88.91	82.80	10.45

Note: # Leads: number of ECG leads used; # Features: number of features extracted. The Se results below 80% are indicated in italics. The best results are indicated in boldface.

learning-based methods, others are feature extraction-based methods. The methods proposed in Refs. 11, 20, 34 and 36 depend on two-lead ECG signals, while the other methods depend on a single ECG lead.

For the deep learning approaches, Ref. 22 used the RBM and the DBN after extracting feature sets, while Ref. 38 developed a 3-layer CNN. For feature extraction, Refs. 11 and 20 consider the RR interval, ECG landmark features such as the QRS duration, T-wave duration, P-wave flag, 2D vectocardiogram loop and others, as their features, while Refs. 34 and 36 consider a combination of landmark and dynamic features, wavelets, ICA and the RR interval as their features. Feature selection is conducted in Ref. 36 to determine the best features. The phase information determined by the synchrosqueezing transform is used as a feature in Ref. 17. In Ref. 7, a random projection is considered to determine the final features. The features of wavelets, local binary patterns, higher-order statistics and several amplitude values with the product, sum and majority rules are employed in Ref. 23. Thereafter, Refs. 11 and 20 select logistic discrimination (LD) as their classifier, while the others select the SVM.

As it can be observed in Table 5, the proposed imbalanced classification model exhibits the best performance in terms of the overall accuracy and the Se of N class. Also, Se of V class performs similarly,  $+P$  of V and F class perform better compared with others. It demonstrates that the extracted features using our proposed time–frequency representation have very good discriminative ability. The poor performance of S class and F class mainly owes to the imbalanced dataset issue. It can be seen from the value of Se and  $+P$  in Table 5, each method has one or more classes with Se below 80%, as the slight improvement in balanced performance is very difficult to achieve. As also shown in Table 5, our balance model achieves the best balanced classification rate. The Se of all beat classes is over 80%, and the overall Acc is also greater than 85%. The result in Ref. 36 is closer to ours, but compared to our results, the Se of S class is below 80%, yet using two leads and additional features. Moreover, they use a complicated feature ranking approach for selecting the features and dimension reduction, which is challenging to implement in real applications.

The balanced results ensure the accuracy of various arrhythmia classifications, while overall accuracy above 85% is clinically acceptable. Moreover, as single-lead and fewer features used, our method can operate on a low-power platform, it offers significant potential to be used in real-time applications in wearable Holters, mobile devices and off-the-person sensors.

## 4. Discussion

### 4.1. Classifier selection

Our extracted features can work with any classifier. To choose a more suitable classifier for ECG signals, we test the widely applied classifiers, including LD,  $k$ -nearest neighbors (kNN), random forest (RF), SVM and NN. These classifiers have



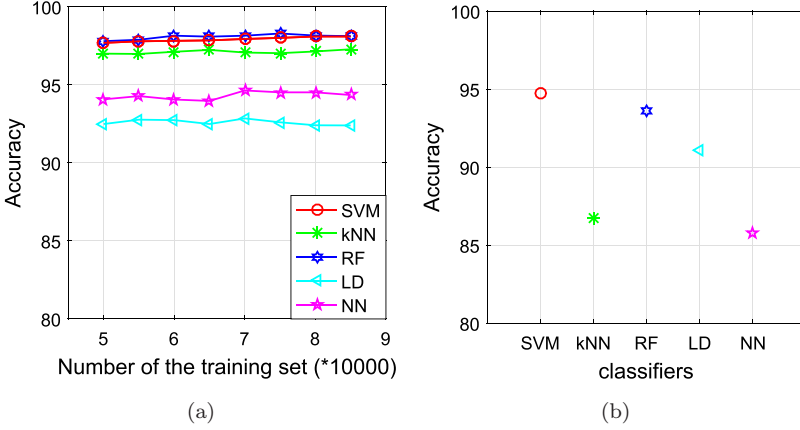


Fig. 7. Comparisons of the accuracy of different classifiers. (a) Heartbeat classification based on intra-patient CV. (b) Heartbeat classification based on inter-patient CV.

been reported as the foremost classifiers for producing high accuracies, particularly in feature extraction-based methods. The performance of these classifiers working with our method is presented in Fig. 7.

It can be seen in Fig. 7(a) that all the tested classifiers achieve the accuracy of the heartbeat classification over 90%, some of them even over 95%, which demonstrate that the extracted features using our proposed time–frequency feature extraction approach have good discriminative ability. Figure 7 shows that RF and SVM exhibit comparable performance of intra-patient CV in (a) and SVM performs better than RF in the inter-patient CV in (b). As the performance of the RF classifier on different data with varying training sample strategies (balanced vs. imbalanced) differs,<sup>24</sup> the differences between various training sample sizes of the SVM classifier are insignificant, besides, ECG data are highly imbalanced and the sample sizes in certain classes are relatively very small, we select the SVM as the classifier in our study.

#### 4.2. Balanced results for improving pathological beats detection

The imbalanced dataset issue is challenging in all automatic heartbeat classification methods. The MIT-BIH arrhythmia database is highly imbalanced, as almost 90% of the beat types belong to the N class. The classification method is prone to ineffective, since it can identify all heartbeats in the N class and achieve a higher overall accuracy, but it neglects the S, V and F classes. However, the main focus of the ECG classification is to identify the S, V and F classes, rather than the N class. In this situation, a more balanced performance result is superior, even with slightly lower accuracy rates in the N class and total average results.

As the purpose of the proposed automatic heartbeat classification is to detect various types of non-lethal arrhythmia, the weighted kernel SVM is considered, and

an extra database, namely the MIT-BIH supraventricular database, is taken into account to address the imbalanced dataset issue. Furthermore, the IF features at other sample points related to the P-wave are extracted to describe the characteristics of the S class, which is conducive to differentiating the S class from the N class. Finally, a classification model with a balanced classification rate is achieved, which specifically exhibits priority over classes with few samples of pathological beats.

#### 4.3. Real-time implementation

The proposed classifier is trained on a computer with 16 GB of RAM and a 2.71 GHz Intel Core i5 processor. The algorithm is developed in MATLAB R2016a. Approximately 81.83s are required to complete one training process. Once the training of ECG signals is complete, the heartbeat classification is rapid. The critical step in the proposed classification system is the feature extraction based on AFD. The computational complexity of the AFD algorithm is  $\mathcal{O}(N \log N)^{13}$  and the computation time of AFD with  $N = 10$  is 0.189s. Note that this time is much shorter than that required to complete one heartbeat, even when the heart rate is as fast as 180 beats per minute. Thus, the proposed algorithm offers potential for real-time monitoring systems, the implementation of which will be the focus of our future work. As none of the methods presented in Table 5 provide the training time, a comparison cannot be conducted. Deep learning approaches require a long training time and specialized hardware, such as a GPU, to train the algorithm efficiently. For example, the CNN in Ref. 2 is trained with two Intel Xeon 2.40 GHz (E5620) processors and 24GB of RAM, requiring approximately 9573.2 s to complete one training epoch, and the total processing time of Ref. 18 is about 1 h on CPU 3.2G Core i7 with 4G memory.

#### 4.4. Limitations and future work

The proposed approach exhibits several limitations. The data are obtained from a publicly available database, and not collected from equipment tailored for telemedicine. Moreover, the database size is limited. Therefore, a larger database collected from professional mobile devices for telemedicine will be executed to confirm the practical performance of the proposed algorithm in follow-up work.

In this study, we focus only on the ECG signal, but the proposed algorithm offers the potential to be applied to other biomedical signals, which will be explored in future work. Furthermore, the possibility of extracting features from AFD to train the deep learning framework and improve the overall performance will be considered in a future study.

### 5. Conclusions

A novel automatic heartbeat classification method based on the recently developed signal processing tool, AFD, which is applied to capture the time-frequency

characteristics of the ECG signal from a complex analysis perspective, has been presented in this paper. The SVM classifier has been considered for automatic classification. The heartbeat classification performance on the MIT-BIH arrhythmia database outperforms other state-of-the-art methods, which depend on a large number of features and/or multi-lead ECG signals, in terms of exhibiting balanced performance and real-time implementation. The balanced results effectively improve pathological detection. The proposed method offers the potential to be used in an ambulatory ECG monitoring device or a mobile health device for real-time diagnosis of non-life-threatening arrhythmia.

## Acknowledgments

This study was supported by the following research grants: The Science and Technology Development Fund of Macao SAR: FDCT 079/2016/A2 and 0123/2018/A3, University of Macau Research Grant: Multiyear 2018-00111-FST.

## References

1. R. M. S. S. Abeysekera and B. Boashash, Time–frequency domain features of ECG signals: Their application in P-wave detection using the cross Wigner–Ville distribution, in *Int. Conf. Acoustics, Speech, and Signal Processing* (IEEE, 1989), pp. 1524–1527.
2. U. R. Acharya *et al.*, A deep convolutional neural network model to classify heartbeats, *Comput. Biol. Med.* **89** (2017) 389–396.
3. A. Alqudah *et al.*, Developing of robust and high accurate ECG beat classification by combining Gaussian mixtures and wavelets features, *Australas. Phys. Eng. Sci. Med.* **42** (2019) 149–157.
4. American National Standard, *Testing and Reporting Performance Results of Cardiac Rhythm and ST-segment Measurement Algorithms*, ANSI/AAMI/ISO EC57, 1998-(R)2008 (American National Standard, 2012).
5. Association for the Advancement of Medical Instrumentation, *Recommended Practice for Testing and Reporting Performance Results of Ventricular Arrhythmia Detection Algorithms* ( Association for the Advancement of Medical Instrumentation, 1987).
6. C. C. Chang and C. J. Lin, LIBSVM: A library for support vector machines, *ACM Trans. Intell. Syst. Technol.* **2** (2017) 1–27, <http://www.csie.ntu.edu.tw/~cjlin/libsvm>.
7. S. Chen *et al.*, Heartbeat classification using projected and dynamic features of ECG signal, *Biomed. Signal Proc. Control* **31** (2017) 165–173.
8. R. R. Coifman and S. Steinerberger, Nonlinear phase unwinding of functions, *J. Fourier Anal. Appl.* **23**(4) (2017) 778–809.
9. R. R. Coifman, S. Steinerberger and H. T. Wu, Carrier frequencies, holomorphy, and unwinding, *SIAM J. Math. Anal.* **49**(6) (2017) 4838–4864.
10. P. Dang, T. Qian and Y. Y. Guo, Transient time–frequency distribution based on mono-component decompositions, *Int. J. Wavelets Multiresolut. Inf. Process.* **11**(3) (2013) 1350022.
11. P. De Chazal, M. O'Dwyer and R. B. Reilly, Automatic classification of heartbeats using ECG morphology and heartbeat interval features, *IEEE Trans. Biomed. Eng.* **51**(7) (2004) 1196–1206.
12. P. Fontana *et al.*, Clinical applicability of a textile 1-lead ECG device for overnight monitoring, *Sensors* **29**(11) (2019) e2436.

13. Y. Gao, M. Ku, T. Qian and J. Wang, FFT formulations of adaptive Fourier decomposition, *J. Comput. Appl. Math.* **324** (2017) 204–215.
14. A. L. Goldberger et al., PhysioBank, PhysioToolkit, and PhysioNet: Components of a new research resource for complex physiologic signals, *Circulation* **101**(23) (2000) e215–e220.
15. P. Guzik and M. Marek, ECG by mobile technologies, *J. Electrocardiol.* **49**(6) (2016) 894–901.
16. A. Y. Hannun et al., Cardiologist-level arrhythmia detection and classification in ambulatory electrocardiograms using a deep neural network, *Nat. Med.* **25**(11) (2019) 65–69.
17. C. L. Herry, M. Frasch, A. J. Seely and H. T. Wu, Heart beat classification from single-lead ECG using the synchrosqueezing transform, *Physiol. Meas.* **38**(2) (2017) 171–187.
18. T. Khatibi and N. Rabinezhadsadatmahaleh, Proposing feature engineering method based on deep learning and  $k$ -NNs for ECG classification and arrhythmia detection, *Australas. Phys. Eng. Sci. Med.* **43** (2020) 49–68.
19. G. Lee et al., Gabor feature extraction for electrocardiogram signals, in *2012 IEEE Biomedical Circuits and Systems Conference (BioCAS)* (IEEE, 2012), pp. 304–307.
20. M. Llamedo and J. P. Martinez, Heartbeat classification using feature selection driven by database generalization criteria, *IEEE Trans. Biomed. Eng.* **58**(3) (2011) 616–625.
21. F. Malmquist, Sur la détermination d’une classe de fonctions analytiques par leurs valeurs dans un ensemble donné de poits, *Comptes Rendues du Sixième Congrès des Mathématiciens Scandinaves (Kopenhagen, 1925)* (Copenhagen, Gjellerups, 1926), pp. 253–259.
22. S. Mathews, C. Kambhamettu and K. E. Barner, A novel application of deep learning for single-lead ECG classification, *Comput. Biol. Med.* **99** (2018) 53–62.
23. V. Mondéjar-Guerra et al., Heartbeat classification fusing temporal and morphological information of ECGs via ensemble of classifiers, *Biomed. Signal Proc. Control* **47** (2019) 41–48.
24. P. T. Noi and M. Kappas, Comparison of random forest,  $k$ -nearest neighbor, and support vector machine classifiers for land cover classification using Sentinel-2 imagery, *Sensors* **18**(1) (2017) 1–20.
25. T. Qian and B. Y. Wang, Adaptive decomposition into basic signals of nonnegative instantaneous frequencies — A variation and realization of Greedy algorithm, *Adv. Comput. Math.* **34**(3) (2010) 279–293.
26. B. Ricaud and B. Torresani, A survey of uncertainty principles and some signal processing applications, *Adv. Comput. Math.* **40**(3) (2014) 629–650.
27. J. Schläpfer and H. J. Wellens, Computer-interpreted electrocardiograms: Benefits and limitations, *J. Am. Coll. Cardiol.* **70**(9) (2017) 1183–1192.
28. S. R. Steinhubl et al., Effect of a home-based wearable continuous ECG monitoring patch on detection of undiagnosed atrial fibrillation: The mSToPS randomized clinical trial, *JAMA* **320**(2) (2018) 146–155.
29. S. Takenaka, On the orthogonal functions and a new formula of interpolation, *Jpn. J. Math.* **2** (1925) 129–145.
30. C. Tan, L. Zhang and H. T. Wu, A novel Blaschke unwinding adaptive-Fourier-decomposition-based signal compression algorithm with application on ECG signals, *IEEE J. Biomed. Health Inf.* **23**(2) (2018) 672–682.
31. V. Vapnik, *The Nature of Statistical Learning Theory* (Springer, 2013).
32. S. S. Virani et al., Heart disease and stroke statistics — 2019 update: A report from the American Heart Association, *Circulation* **141** (2020) e139–e596.

33. H. T. Wu, J. C. Wu, P. C. Huang, T. Y. Lin, T. Y. Wang, Y. H. Huang and Y. L. Lo, Phenotype-based and self-learning inter-individual sleep apnea screening with a level IV-like monitoring system, *Front. Physiol.* **9** (2018) 723.
34. C. Ye, B. V. K. Vijaya Kumar and M. Coimbra, Heartbeat classification using morphological and dynamic features of ECG signals, *IEEE Trans. Biomed. Eng.* **59**(10) (2012) 2930–2941.
35. Ö. Yildirim, A novel wavelet sequence based on deep bidirectional LSTM network model for ECG signal classification, *Comput. Biol. Med.* **96** (2018) 189–202.
36. Z. Zhang *et al.*, Heartbeat classification using disease-specific feature selection, *Comput. Biol. Med.* **46** (2014) 79–89.
37. L. Zhang, T. Qian, W. Mai and P. Dang, Adaptive Fourier decomposition-based Dirac type time–frequency distribution, *Math. Methods Appl. Sci.* **40**(8) (2017) 2815–2833.
38. M. Zubair, J. Kim and C. Yoon, An automated ECG beat classification system using convolutional neural networks, in *2016 6th Int. Conf. IT Convergence and Security (ICITCS)* (IEEE, 2016), pp. 1–5.

Copyright of International Journal of Wavelets, Multiresolution & Information Processing is the property of World Scientific Publishing Company and its content may not be copied or emailed to multiple sites or posted to a listserv without the copyright holder's express written permission. However, users may print, download, or email articles for individual use.